Journal of Luminescence 128 (2008) 1937–1941

Contents lists available at ScienceDirect

Journal of Luminescence

journal homepage: www.elsevier.com/locate/jlumin

Spectral-kinetic characteristics of Pr^{3+} luminescence in $LiLuF_4$ host upon excitation in the UV–VUV range

G. Stryganyuk [a,b,*], G. Zimmerer [a,c], N. Shiran [d], V. Voronova [d], V. Nesterkina [d], A. Gektin [d], K. Shimamura [e], E. Villora [e], F. Jing [e], T. Shalapska [b], A. Voloshinovskii [b]

[a] HASYLAB at DESY, Notkestr. 85, 22607 Hamburg, Germany
[b] Ivan Franko National University of Lviv, 8 Kyryla i Mefodiya Str., 79005 Lviv, Ukraine
[c] Institute of Experimental Physics, University of Hamburg, Luruper Chaussee 149, 22761 Hamburg, Germany
[d] Institute for Scintillation Materials, 60 Lenin Avenue, 61001 Kharkov, Ukraine
[e] Advanced Materials Laboratory, National Institute for Materials Science, 1-1 Namiki, Tsukuba, Ibaraki 305-0044, Japan

ARTICLE INFO

Article history:
Received 7 February 2008
Received in revised form
14 April 2008
Accepted 3 June 2008
Available online 7 June 2008

PACS:
78.55.Hx

Keywords:
Pr^{3+} luminescence
Cross-relaxation
Luminescence decay kinetics
$LiLuF_4$

ABSTRACT

Spectral-kinetic study of Pr^{3+} luminescence has been performed for $LiLuF_4$:Pr(0.1 mol%) single crystal upon the excitation within 5–12 eV range at $T = 8$ K. The fine-structure of Pr^{3+} 4f ^{2}→4f 5d excitation spectra is shown for $LiLuF_4$:Pr(0.1 mol%) to be affected by the efficient absorption transitions of Pr^{3+} ions into 4f 5d involving 4f ^{1} core in the ground state. Favourable conditions have been revealed in $LiLuF_4$:Pr(0.1 mol%) for the transformation of UV–VUV excitation quanta into the visible range. Lightly doped $LiLuF_4$:Pr crystals are considered as the promising luminescent materials possessing the efficient Pr^{3+} $^3P_0$ visible emission upon UV–VUV excitation. The mechanism of energy transfer between Lu^{3+} host ion and Pr^{3+} impurity is discussed.

1. Introduction

The luminescent characteristics of Pr^{3+} doped fluorides show rather attractive prospects in lighting applications [1–4], development of fast scintillators [5] and tuneable UV–VUV laser sources [6]. Single crystals of $LiYF_4$ and $LiLuF_4$ have been extensively studied as the wide band-gap hosts for trivalent rare earth (RE^{3+}) ions. These crystals have a tetragonal structure with C^6_{4h} space group and provide the single site of S_4 symmetry for RE^{3+} ion at Y^{3+} or Lu^{3+} sites [7,8].

The intraconfigurational Pr^{3+} 4f ^{2} transitions have thoroughly been studied for $LiYF_4$:Pr^{3+} [9], whereas the simulation of Pr^{3+} 4f 5d states fails to reproduce accurately the experimental data and the origin of structure in Pr^{3+} 4f ^{2}→4f 5d excitation spectra is not quite clear up to now. This difficulty is common in study of 4f ^{N}→4f $^{N-1}$ 5d transitions for all RE^{3+} ions since the extended 5d orbits undergo the electron–phonon interaction causing the vibronic bands that complicates the spectra analysis. However, the recent calculations for $4f^N \rightarrow 4f^{N-1}$ 5d transitions of RE^{3+} ions in $LiYF_4$ [10–13] show rather good agreement with experimental results. Present paper reports on the time-resolved high-resolution (3.2–0.6 Å) study of Pr^{3+} luminescence in $LiLuF_4$:Pr(0.1 mol%) single crystal upon the excitation within 5–12 eV range at $T = 8$ K.

2. Experiment details

Scheelite $LiLuF_4$:Pr single crystal was grown from platinum crucible using Czochralski technique with the growth conditions modified according to the previous investigations [14]. Resistive high-purity graphite heater was used. The starting charge was prepared from commercial LiF, LuF_3 and PrF_3 powders of high purity (>99.99%). The concentration of Pr^{3+} in the starting charge was adjusted to 1 mol%. The growth system was preheated at 700 °C and pumped down to 10^{-5} mbar for 12 h to eliminate water and oxygen from the growth chamber and starting charge. Thereafter, the growth chamber was slowly filled with a pure (99.9999%) CF_4 gas and the charge was melted at approximately 820 °C. $LiLuF_4$:Pr(0.1 mol%) sample of $10 \times 10 \times 1$ mm^3 size was cut from the central part of the grown bulk in (0 0 1) plain

* Corresponding author. SRC Carat, Institute for Materials, 202 Stryjska Str., 79031 Lviv, Ukraine. Tel.: +38 032 294 9731.
E-mail address: stryganyuk@gmail.com (G. Stryganyuk).

0022-2313/$ - see front matter © 2008 Elsevier B.V. All rights reserved.
doi:10.1016/j.jlumin.2008.06.003

perpendicular to *c*-axis. Chemical composition was determined by the inductively coupled plasma method.

Measurements of luminescence excitation and emission spectra as well as luminescence decay kinetics were performed at Deutsches Elektronen Synchotron (DESY, Hamburg) using the synchrotron radiation from DORIS III storage ring and facility of SUPERLUMI experiment at HASYLAB [15]. Helium flow-type cryostat has been used to stabilize the temperature at $T = 8$ K. Time-integrated emission spectra were measured with the spectral resolution of about 0.3 nm using 0.3 m ARC "Spectra Pro 308" monochromator-spectrograph in Czerny-Turner mounting equipped with 300, 1200 groves/mm gratings and Princeton Instruments CCD detector (1100×300 pixels). The emission spectra were not corrected for the spectral sensitivity of the detection system, i.e., the real relative intensity can differ from that in presented emission spectra. Time-resolved luminescence excitation spectra were scanned with the resolution of 3.2–0.6 Å within 5–12 eV range by the primary 2 m monochromator in 15° McPherson mounting (equipped with Jobin Yvon holographic concave grating, Al+MgF_2 coating, 1200 groves/mm) using HAMAMATSU R6358P photomultiplier at the secondary ARC monochromator. Spectra of the fast emission component were registered after the excitation pulse within 2–8 ns time-gate, slow component—within 120–190 ns one. Time-integrated spectra correspond to the total signal from the photomultiplier. The primary monochromator was calibrated with ±0.05 Å accuracy using $^1S_0 \rightarrow {}^3P_j$ absorption of atomic xenon and krypton gases as a reference in 115–147 nm range. Luminescence excitation spectra have been corrected on the incident photon flux. Luminescence decay kinetics was registered within 200 ns time gate defined by the excitation pulse repetition upon the storage ring operation in five bunch mode. Microcal Origin software has been used to determine the decay–time constant for the main decay component assuming its exponential profile.

3. Experimental results and discussion

The emission spectra of $LiLuF_4$:Pr(0.1 mol%) crystal measured upon the different excitation energies at $T = 8$ K within 200–800 nm range are presented in Fig. 1. Emission in four structured bands within 216–266 nm range (Fig. 1) reveals the excitation threshold at 5.73 eV (Fig. 2(a)) and the dominant fast component (Fig. 2(a), curve 2) with 22 ns decay–time constant (Fig. 3, curve 2) upon the excitation up to 8.3 eV. Such spectral-kinetic characteristics prove 216–266 nm emission to originate mainly from the dipole-allowed 4f 5d→4f ^{2} radiative transitions of impurity Pr^{3+} ions in $LiLuF_4$ host [16]. Fine structure of Pr^{3+} 4f 5d→4f ^{2} emission spectrum (Fig. 4) reproduces well the detailed diagram of low-lying energy levels of Pr^{3+} in $LiLuF_4$ host [8–17]. The excitation bands (A, B, C and D) within 5.73–8.3 eV (Fig. 2) correspond to the interconfigurational 4f ^{2}→4f 5d transitions of Pr^{3+} ion [12].

Observation of fast Pr^{3+} 4f 5d→4f ^{2} luminescence implies the absence of energy gap between Pr^{3+} $^1S_0$ level and 4f 5d band [1]. However, 410 nm emission shows the same excitation features as 4f 5d→4f ^{2} luminescence in 5.73–8.5 eV range (Fig. 2(b)) but possesses relatively slow (about 1 μs) decay component (Fig. 3(b)) that is characteristic for Pr^{3+} $^1S_0 \rightarrow {}^1I_6$ transitions [4]. Thus, the emission around 410 nm may originate from both 4f 5d and $^1S_0$ states of Pr^{3+}, whereas the contribution of 4f 5d→4f ^{2} radiative transitions prevails within 216–266 nm range.

Excitation spectra of the emission originating from Pr^{3+} $^3P_0$ show the distinct excitation maximum A_0 at 5.72 eV (Fig. 2(c))

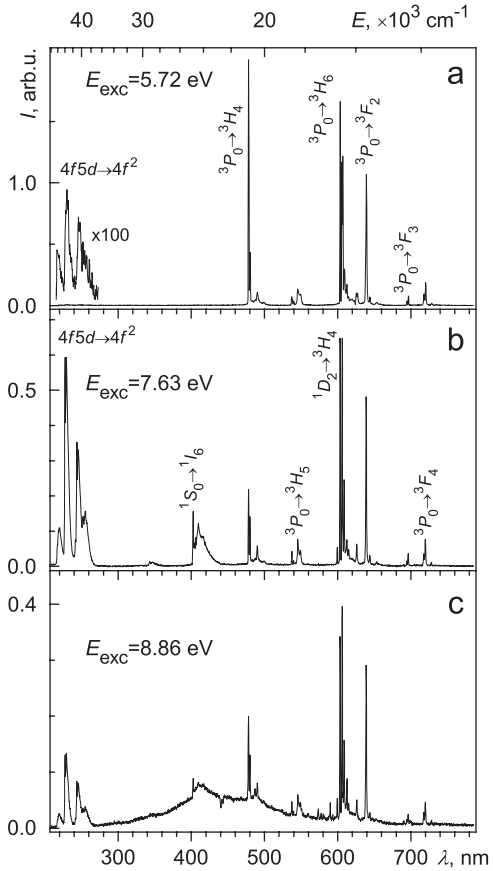

Fig. 1. Time-integrated emission spectra of $LiLuF_4$:Pr(0.1 mol%) single crystal measured upon different excitation energies at $T = 8$ K.

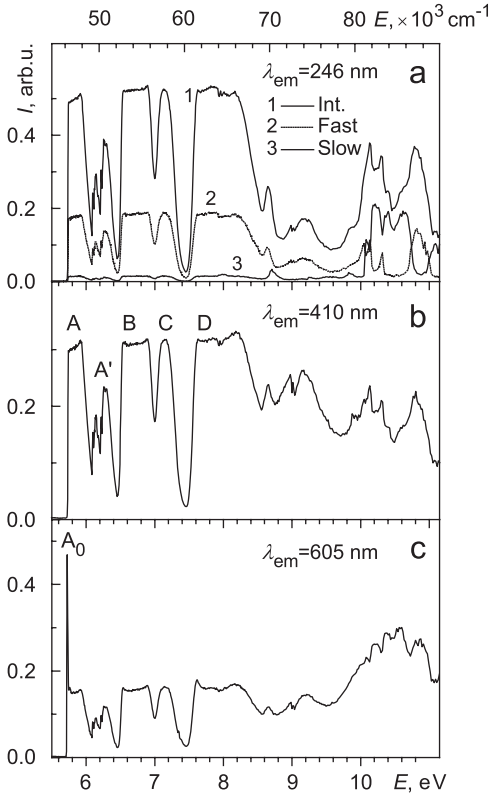

Fig. 2. Time-resolved (a) and time-integrated (b, c) excitation spectra of $LiLuF_4$:Pr(0.1 mol%) luminescence measured at $T = 8$ K with the resolution interval of 3.2 Å.

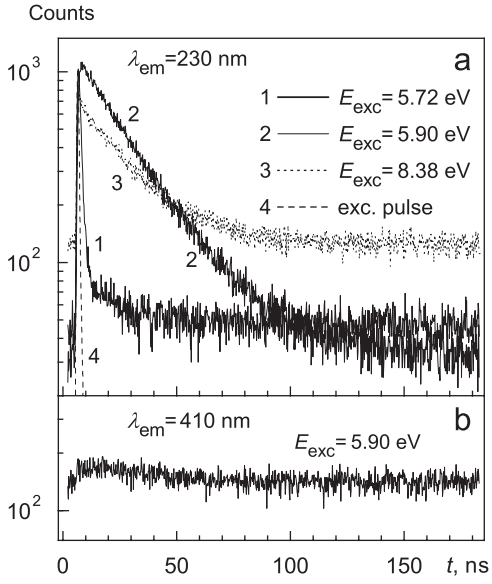

Fig. 3. Decay kinetics of emission at 230 (a) and at 410 nm (b) from $LiLuF_4$:Pr(0.1 mol%) single crystal. $T = 8$ K. Excitation pulse (120 ps) is reproduced by the registration system as the decay profile with 0.4 ns time constant (dashed line 4).

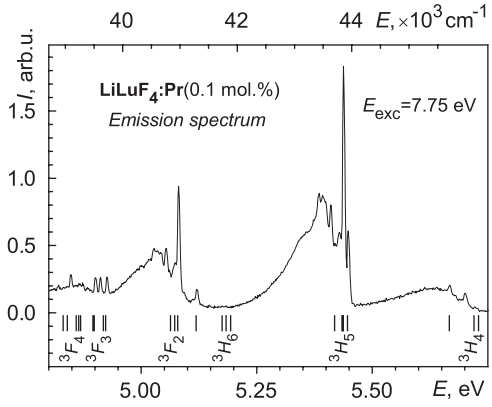

Fig. 4. Time-integrated emission spectrum of $LiLuF_4$:Pr(0.1 mol%) single crystal upon 7.75 eV excitation at $T = 8$ K. The diagram of low-lying energy levels of Pr^{3+} in $LiLuF_4$ host [8–17] is presented below.

which is not observed for 4f 5d→4f ^{2} and $^1S_0$ emission (Figs. 2(a) and (b)). Upon the excitation at 5.72 eV, Pr^{3+} $^3P_0$ emission dominates (Fig. 1(a)) and shows the intensity higher than upon other excitation probed (Fig. 2(c)). On the contrary, the emission intensity in 4f 5d→4f ^{2} bands is extremely low (Fig. 1(a)) and respective decay kinetics (Fig. 3(a), curve 1) shows a very fast component (with 1.3 ns time constant) upon 5.72 eV excitation. One may conclude the nonradiative relaxation of Pr^{3+} 4f 5d states upon the excitation at 5.72 eV.

Fig. 5 shows the detailed spectral features of 4f 5d→4f ^{2} and $^3P_0 \rightarrow {}^3H_4$ luminescence within 5.63–5.77 eV range. The overlap of 4f 5d→4f ^{2} emission spectrum with the excitation spectrum of $^3P_0 \rightarrow {}^3H_4$ luminescence shows up within 5.72–5.73 eV range where the zero-phonon 4f 5d↔4f ^{2} transitions are expected. The intensity of zero-phonon line (ZPL) in the emission spectrum (curve 1) may be reduced due to the reabsorption. Maxima of $^3P_0 \rightarrow {}^3H_4$ luminescence excitation (curve 2, around 5.72 and 5.73 eV) appear to be well matched with two lowest Stark levels of Pr^{3+} $^3H_4$ state (vertical ticks in Fig. 5) positioned for their best fit with emission maxima (see Fig. 4). However, it is rather strange to have a higher intensity from the second Stark component (tick at

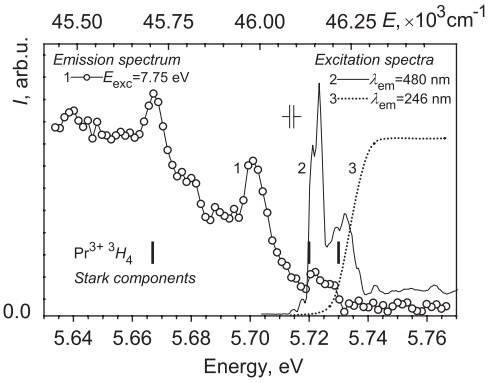

Fig. 5. Emission spectrum of $LiLuF_4$:Pr(0.1 mol%) single crystal upon 7.75 eV excitation (circled curve 1) presented together with the excitation spectra of 480 nm (solid curve 2) and 246 nm (dotted curve 3) emission at $T = 8$ K. The Stark components of Pr^{3+} $^3H_4$ in $LiLuF_4$ host [8–17] are shown with the vertical ticks. Resolution interval is presented for the excitation spectra (vertical slit mark).

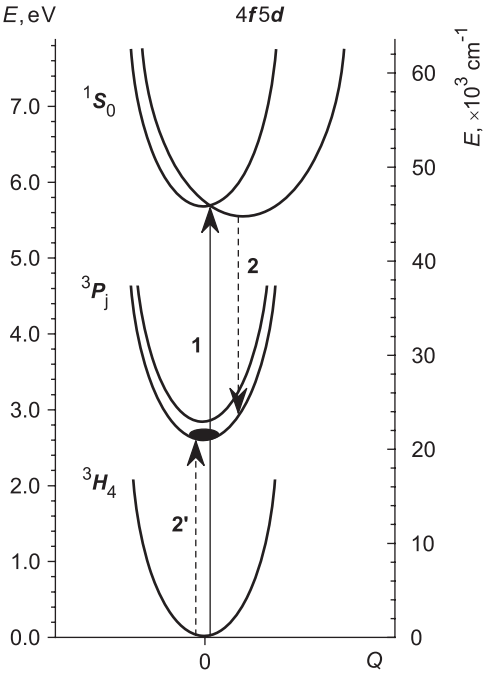

Fig. 6. Configurational coordinate diagram for Pr^{3+} elucidating the hypothetical cross-relaxation processes (transitions 2, 2′) in $LiLuF_4$:Pr(0.1 mol%) single crystal after 4f ^{2}→4f 5d excitation (transitions 1) at $T = 8$ K.

5.72 eV) which has the population probability of a few orders lower than one of the lowest Pr^{3+} $^3H_4$ level (tick at 5.73 eV).

Fig. 6 shows the hypothetical mechanism of $^3P_0$ population upon the excitation of Pr^{3+} into the lowest 4f 5d states ($E_{exc} = 5.73$ eV, transition 1). The broadening and slow decay kinetics of 410 nm emission band allow us to relate its origin with both $^1S_0$ and 4f 5d states implying their relative location presented in a configurational coordinate diagram (Fig. 6). The energy positions of Pr^{3+} $^3H_4$, ^3P_j, $^1S_0$ levels and lowest 4f 5d state have been adjusted according to the literature data [8–17] and spectral characteristics of $LiLuF_4$:Pr(0.1 mol%) emission presented in this work. The suggested location of lowest 4f 5d state and ^3P_j levels of Pr^{3+} in $LiLuF_4$:Pr(0.1 mol%) allows the cross-relaxation (Fig. 6, transitions 2, 2′) between neighbour Pr^{3+} ions:

$$4f\ 5d + {}^3H_4 \rightarrow {}^3P_0 + {}^3P_0 \quad (1)$$

In a very narrow 5.72–5.73 eV energy range, the interconfigurational Pr^{3+} 4f ^{2}→4f 5d absorption is still low (Fig. 5, curve 3) and the large penetration depth of excitation quanta provides the efficient excitation of Pr^{3+} ion in the volume of $LiLuF_4$:Pr(0.1 mol%) crystal. Thus, excitation of $LiLuF_4$:Pr(0.1 mol%) into the lowest Pr^{3+} 4f 5d states leads to (i) the efficient excitation of Pr^{3+} impurity due to the deep penetration of excitation quanta, (ii) subsequent decay of Pr^{3+} 4f 5d states via the cross-relaxation (1) followed by (iii) emitting of visible quanta by pairs of neighbour Pr^{3+} ions.

The similar processes of UV–VUV photon cutting may occur upon the excitation into the higher Pr^{3+} 4f 5d states, but their luminescent output (Pr^{3+} $^3P_0$ emission) comes to be considerably lower because of the reduced number of Pr^{3+} pair in the excited crystal volume due to the small penetration of the excitation quanta in the range of efficient 4f ^{2}→4f 5d absorption. The efficiency of Pr^{3+} $^3P_0$ emission is affected already at 5.73 eV (Fig. 5, curve 2) by the decrease of penetration depth due to the intensification of 4f ^{2}→4f 5d absorption (Fig. 5, curve 3) and the height of excitation maximum at 5.72 eV originating from the second Stark component of $^3H_4$ state exceeds that of one at 5.73 eV originating from the lowest $^3H_4$ level. Splitting of about 2–3 meV revealed for the main maxima of 4f 5d absorption within 5.72–5.74 eV (Fig. 5, curve 2) has most probably a phonon-related origin.

One may expect the excitation efficiency of Pr^{3+} $^3P_0$ emission to be a few orders higher at 5.73 eV (compare with 5.72 eV one) for a lightly doped $LiLuF_4$:Pr crystal where the excitation quanta are not absorbed within a thin outer layer but penetrate deep into the crystal. Of course, the decrease of Pr^{3+} content reduces the cross-relaxation processes and the intensity of $^3P_0$ luminescence consequently, but there should be an optimal Pr^{3+} concentration providing the maximal efficiency of Pr^{3+} $^3P_0$ emission due to UV photon cutting (1).

Four bands (A, B, C and D) of Pr^{3+} 4f ^{2}→4f 5d absorption (Fig. 2) prevail in the excitation spectra of emission from Pr^{3+} 4f 5d and $^1S_0$ (frames a, b). These bands show up also in the excitation spectra of Pr^{3+} $^3P_0$ emission (Fig. 2(c)) but with the intensity lower than one in A_0 maxima (5.72–5.73 eV). The saturation effect is pronounced for Pr^{3+} 4f ^{2}→4f 5d excitation in $LiLuF_4$:Pr(0.1 mol%) as a confined luminescence efficiency in A, B, C and D bands due to the absorption of excitation quanta within a thin outer layer of the crystal where the nonradiative decay of Pr^{3+} 4f5d states appears because of their interaction with the surface defects.

Upon the excitation above 8.3 eV, Pr^{3+} $^3P_0$ emission reveals relatively higher intensity (Fig. 2(c)) compare to the case of emission from Pr^{3+} 4f 5d and $^1S_0$ states (Figs. 2(a, b)). This may be explained by the higher efficiency of Pr^{3+} $^3P_0$ population via the energy transfer from excitonic states or recombination of Pr^{3+} with electron–hole pairs [18,19]. A broad band within 300–550 nm arises in the emission spectrum of $LiLuF_4$:Pr(0.1 mol%) upon the excitation at 8.86 eV (Fig. 1(c)). This band has most likely the intrinsic origin and corresponds to the excitonic emission of $LiLuF_4$ host.

Fine structure in A′ band (6.08–6.43 eV) is revealed for all measured excitation spectra of Pr^{3+} emission (Fig. 2). Fine structure in 4f ^{N}→4f $^{N-1}$ 5d excitation spectra of RE^{3+} ions has been assigned to the excited 4f $^{N-1}$ 5d states involving 5d electron in the lowest crystal-field level and 4f $^{N-1}$ core in an excited state [20]. Fig. 7 presents a detailed structure in A′ excitation band revealed for Pr^{3+} emission in $LiLuF_4$:Pr(0.1 mol%). A′ band shows a clearly resolved doublet of excitation peak series with the first maxima at 6.093 eV (A'_1) and 6.215 eV (A'_2). These two A′ series originate most likely from different 5d electron states. The energy distance of 0.36 eV between A'_1 maximum (6.215 eV) and the lowest Pr^{3+} 4f 5d state (5.730 eV) is different from the known

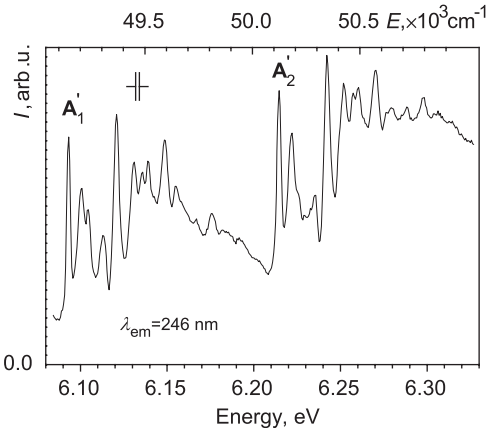

Fig. 7. High-resolution excitation spectra of Pr^{3+} 4f 5d→4f ^{2} emission from $LiLuF_4$:Pr(0.1 mol%) single crystal measured within the range of Pr^{3+} 4f ^{2}→4f 5d absorption at $T = 8$ K. The resolution interval is presented by the vertical slit mark.

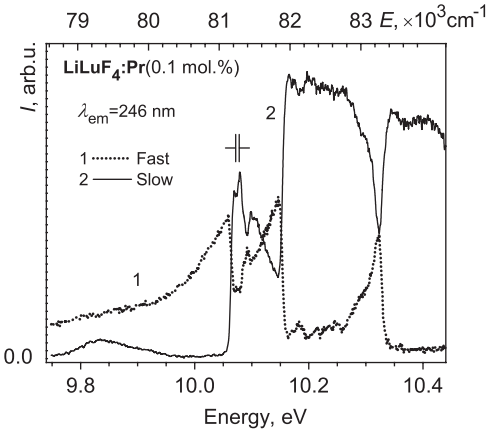

Fig. 8. High-resolution time-resolved excitation spectra of Pr^{3+} 4f 5d→4f ^{2} emission from $LiLuF_4$:Pr(0.1 mol%) single crystal measured within the range of Lu^{3+} 4f ^{14}→4f ^{13}5d absorption at $T = 8$ K.

splitting of 4f ^{1} core (about 0.25 eV) because of f–d interaction in the excited 4f 5d state [12].

The decay kinetics of Pr^{3+} 4f 5d→4f ^{2} emission shows the rise of slow component (~100 μs time constant) upon the excitation above 8.3 eV (Fig. 3(a), curve 3). The competition between the fast and slow mechanisms of Pr^{3+} excitation is clearly observed in the excitation spectra of Pr^{3+} 4f 5d→4f ^{2} emission above 10 eV (Fig. 2(a), curves 2, 3). Fig. 8 presents the high-resolution excitation spectra for the fast (curve 1) and slow (curve 2) components of 4f 5d→4f ^{2} emission ($\lambda_{em} = 246$ nm). Excitation spectrum of slow emission component reproduces the absorption of Lu^{3+} host ions due to the spin-forbidden (10.06 eV threshold) and spin-allowed (10.15 eV threshold) Lu^{3+} 4f ^{14}→4f ^{13}5d transitions [13]. Lu^{3+} 4f ^{13}5d→4f ^{14} emission (9.85–10.05 eV) is known to be due to the spin-forbidden radiative transition at $T = 8$ K and has a characteristic slow decay kinetics. Thus, the energy transfer between Lu^{3+} and Pr^{3+} occurs via the reabsorption of Lu^{3+} 4f ^{13}5d→4f ^{14} emission by Pr^{3+} ions giving rise to the slow component of Pr^{3+} 4f 5d→4f ^{2} luminescence.

4. Conclusions

Spectral-kinetic study of Pr^{3+} luminescence in $LiLuF_4$:Pr(0.1 mol%) single crystals at $T = 8$ K has shown the emission around 410 nm to originate from both 4f 5d and $^1S_0$ states of Pr^{3+} and the

main contribution of radiative Pr^{3+} 4f 5d→4f ^{2} transitions into the emission within 216–266 nm range.

In the case of studied $LiLuF_4$:Pr(0.1 mol%) single crystal, the fine structure of Pr^{3+} 4f ^{2}→4f 5d excitation spectra is affected at $T = 8$ K by the efficient absorption transitions of Pr^{3+} into 4f 5d involving 4f ^{1} core in the ground state. $LiLuF_4$:Pr(0.1 mol%) possesses a favourable conditions for the transformation of excitation UV–VUV quanta into the visible range via the cross-relaxation processes involving neighbour Pr^{3+} ions. The relaxation of excited Pr^{3+} ions within the lowest well-defined 4f 5d states occurs in $LiLuF_4$:Pr(0.1 mol%) via the cross-relaxation resulting in the population of Pr^{3+} $^3P_0$ states. Excitation of Pr^{3+} ion into the lowest 4f 5d state leads to (i) the efficient excitation of the Pr^{3+} impurity due to the deep penetration of excitation quanta, (ii) subsequent decay of Pr^{3+} 4f 5d states via the cross-relaxation (4f 5d+$^3H_4$→$^3P_0$+$^3P_0$) followed by (iii) emitting of visible quanta by pairs of neighbour Pr^{3+} ions. The efficiency of such cross-conversion depends on the concentration of Pr^{3+} impurity, and may be affected by the reduced penetration of excitation quanta due to the efficient Pr^{3+} 4f ^{2}→4f 5d absorption in the outer layer of the crystal with a high content of Pr^{3+}. Lightly doped $LiLuF_4$:Pr crystal with optimal Pr^{3+} concentration may be considered as a promising luminescent material (with quantum yield greater than 1) possessing the efficient Pr^{3+} $^3P_0$ visible emission upon UV–VUV photon absorption. However, the tentative study of $LiLuF_4$:Pr luminescence at room temperature is still desirable.

The energy transfer between Lu^{3+} host ion and Pr^{3+} impurity occurs in $LiLuF_4$:Pr(0.1 mol%) via the reabsorption of Lu^{3+} 4f ^{13}5d→4f ^{14} emission by Pr^{3+} ions giving rise to the slow component of Pr^{3+} 4f 5d→4f ^{2} emission upon the excitation above 10 eV.

Acknowledgements

The valuable comments of Prof. Andries Meijerink (Utrecht University, the Netherlands) are gratefully acknowledged. Authors also appreciate the support of Superlumi experiment by HASYLAB (DESY, Hamburg).

References

[1] W.W. Piper, J.A. DeLuca, F.S. Ham, J. Lumin. 8 (1974) 344.
[2] R.T. Weg, H. Donker, K.D. Oskam, A. Meijerink, Science 283 (1999) 664.
[3] E. van der Kolk, P. Dorenbos, C.W.E. van Eijk, et al., J. Lumin. 97 (2002) 212.
[4] S. Kuck, I. Sokolska, M. Henke, T. Scheffler, E. Osiac, Phys. Rev. B 71 (2005) 165112.
[5] W. Drozdowski, A.J. Wojtowicz, J. Alloys Compds. 300–301 (2000) 261.
[6] S. Nicolas, E. Descroix, M.-F. Joubert, et al., Opt. Mater. 22 (2003) 139.
[7] E. Garcia, R.R. Ryan, Acta Cryst. C 49 (1993) 2053.
[8] A.A. Kaminskii, Phys. Status Solidi A 97 (1986) K53.
[9] L. Esterowitz, F.J. Bartoli, R.E. Allen, et al., Phys. Rev. B 19 (1979) 6442.
[10] M. Laroche, J.-L. Doualan, S. Girard, et al., J. Opt. Soc. Amer. B 17 (2000) 1291.
[11] M.F. Reid, L. van Pieterson, R.T. Weg, A. Meijerink, Phys. Rev. B 62 (2000) 14744.
[12] L. van Pieterson, et al., Phys. Rev. B 65 (2002) 45113.
[13] M. Kirm, G. Stryganyuk, S. Vielhauer, G. Zimmerer, V.N. Makhov, B.Z. Malkin, O.V. Solovyev, R. Yu Abdulsabirov, S. Lkorableva, Phys. Rev. B 75 (2007) 075111.
[14] K. Shimamura, H. Sato, A. Bensalah, et al., Cryst. Res. Technol. 36 (2001) 801.
[15] G. Zimmerer, Radiat. Meas. 42 (2007) 859.
[16] E. Sarantopoulou, A.C. Cefalas, M.A. Dubinskii, et al., Opt. Lett. 19 (1994) 499.
[17] S. Nicolas, E. Descroix, Y. Guyot, M.-F. Joubert, et al., Opt. Mater. 16 (2001) 233.
[18] P.A. Rodnyi, P. Dorenbos, G.B. Stryganyuk, et al., J. Phys. Condens. Matter 15 (2003) 719.
[19] A.P. Vink, P. Dorenbos, CWE. van Eijk, J. Solid State Chem. 171 (2003) 308.
[20] L. van Pieterson, M.F. Reid, A. Meijerink, Phys. Rev. Lett 88 (2002) 67405.